NJC

Accepted Manuscript

This is an *Accepted Manuscript*, which has been through the Royal Society of Chemistry peer review process and has been accepted for publication.

Accepted Manuscripts are published online shortly after acceptance, before technical editing, formatting and proof reading. Using this free service, authors can make their results available to the community, in citable form, before we publish the edited article. We will replace this *Accepted Manuscript* with the edited and formatted *Advance Article* as soon as it is available.

You can find more information about *Accepted Manuscripts* in the Information for Authors.

Please note that technical editing may introduce minor changes to the text and/or graphics, which may alter content. The journal's standard Terms & Conditions and the Ethical guidelines still apply. In no event shall the Royal Society of Chemistry be held responsible for any errors or omissions in this *Accepted Manuscript* or any consequences arising from the use of any information it contains.

ROYAL SOCIETY OF CHEMISTRY

www.rsc.org/njc

New Journal of Chemistry RSCPublishing

ARTICLE

Synthesis and Characterization of Two Novel Dicyanidoargentate(I) Complexes Containing N-(2-hydroxyethyl)ethylenediamine Exhibiting Considerable Biological Activity

Cite this: DOI: 10.1039/x0xx00000x

Received 00th January 2012,
Accepted 00th January 2012

DOI: 10.1039/x0xx00000x

www.rsc.org/

Nesrin Korkmaz[a], Ahmet Karadağ[a*], Ali Aydın[b], Yusuf Yanar[c], İsa Karaman[d] and Şaban Tekin[b]

Two novel cyanido-bridged bimetallic polymeric complexes, $[Ni(hydeten)_2Ag(CN)_2][Ag(CN)_2].H_2O$ (***C1***) and $[Cd_2(hydeten)_2Ag_4(CN)_8].H_2O$ (***C2***) (*hydeten*: N-(2-hydroxyethyl) ethylenediamine) were synthesized and characterized by elemental, FT-IR, X-Ray (***C2***), thermal and variable temperature magnetic measurement (***C1***) techniques. Anticancer, antibacterial and antifungal effects were also investigated. The crystallographic analyses showed that ***C2*** crystallizes in monoclinic space group P21/c and shows a *3D* 6,4 ladder-type polymeric chain in which the Cd^{II} centers are linked by $[Ag(CN)_2]^-$ units. The Ag...Ag distances exhibit short value of 3.1365(9) Å. It features rare linear pentameric unit of $[Ag(CN)_2]^-$ ions assembled by d^{10}–d^{10} interaction as building blocks. Both complexes exhibited outstanding antibacterial, antifungal and anticancer activities against ten different bacterial strains, two plant pathogenic fungi (*Alternaria solani* and *Rhizoctonia solani*) and four tumor cell lines (*HT-29*, *HeLa*, *C6* and Vero), respectively.

I. Introduction

In inorganic coordination polymers, the choice of metal/ligand combination is the main factor to help control both the supramolecular topology and dimensionality. Additionally, other forces such as hydrogen-bonding, π–π interactions, metal–metal interactions can also greatly influence the crystal structure and its dimensionality [1-3]. Among these polymers, Ag^I coordination polymers are of great interest because the Ag–donor atom bond shows the high lability and the resulting Ag^I coordination polymers can generally be crystallized allowing investigation by X-ray diffraction [4-6]. On the other hand, Ag^I ions are known to show a tendency to form the silver–silver bonds which could be used to control supramolecular structure and dimensionality [7].

Dicyanidoargentate, $[Ag(CN)_2]^-$, is a linear anion, of considerable stability and simplicity. Also, this anion has significant importance in practical applications and fundamental chemical behaviors [8, 9]. It is well-known that cyano groups in cyanidometalates units such as $[Ag(CN)_2]^-$ can act as bridging ligands and a polymeric structure can be formed through Ag-Ag (argentophilic) interactions. This property has been explored in the construction of many oligomeric and polymeric structures with different dimensionalities [10]. Ag^I complexes are also known to self-associate through analogous argentophilic interactions [11]. Argentophilic interactions are characteristic of $[Ag(CN)_2]^-$ [12-17] and a typical range for these Ag…Ag contacts are ca. 3.05- 3.26 Å, but both shorter [2.9879(9) Å] [13] and longer [3.899(1) Å] [15] contacts have been reported, too.

$[Ag(CN)_2]^-$ complexes have many practical applications in various fields. Industrially, $[Ag(CN)_2]^-$ is utilized in electroplating processes. In medicine, $[Ag(CN)_2]^-$ is used as a bactericide [8,9]. The varieties of $[Ag(CN)_2]^-$ with a diamagnetic cadmium atom have recently attracted the attention of Iwamoto's research group [13,14,16,18,19]. On the other hand, little attention has been paid to the low-dimensional $[Ag(CN)_2]^-$ with paramagnetic central atoms. These have been mainly investigated from the structural and magneto chemical point of view but the thermal stability and stoichiometry associated with their thermal decomposition have been studied only to a lesser extent [12, 20-26].

Hydeten, (N-(2-hydroxyethyl)-ethylenediamine; alternatively named 2-(2-aminoethylamino)-ethanol ,$H_2NCH_2CH_2NHCH_2CH_2OH$, was used in this study as a ligand coordinated to a metal ion through its three donor atoms. Karadağ et. al observed two different coordination modes of the *hydeten* ligand. In these studies, *hydeten* acted as a bidentate ligand through its two nitrogen donor sites [27-31] and a tridentate ligand via its all three donor centers [32].

The discovery of the anticancer potential of *cis*platin led to the development of a new class of metallo-drugs. Several platinium

based metal complexes; carboplatin and oxaliplatin have been used succesfully as anticancer drugs. There are other metallo drug candidates containing other metals such as rutenium and gallium under investigation. Their extremely diverse structural chemistry and interaction of metals with biomolecules such as DNA, RNA and proteins result in the exploration of biological activities of other metal coordination complexes with anticancer, antibacterial, antifungal and antiviral drug potential. In the present study, biological activities of two novel dicyanidoargentate(I) complexes containing N-(2-hydroxyethyl)ethylenediamine were investigated.

In this study, $[Ni(hydeten)_2Ag(CN)_2][Ag(CN)_2].H_2O$ (***C1***) and $[Cd_2(hydeten)_2Ag_4(CN)_8].H_2O$ (***C2***) were successfully synthesized and characterized by elemental analysis, FT-IR, thermal analysis, magnetic analysis and X-ray crystallography. In addition antibacterial, antifungal, anticancer activities and mechanism of actions of ***C1*** and ***C2*** were determined for the first time.

II. Experimental

2.1. Materials and instrumentation

$AgNO_3$, $CdSO_4.8/3H_2O$, $NiCl_2.6H_2O$, KCN and N-(2-hydroxyethyl)-ethylenediamine (*hydeten*) were used as received.

Elemental analyses (C, H and N) were performed using a LECO CHNS-932 elemental analyzer. IR spectra were measured on a Jasco 430 FT-IR spectrometer using KBr pellets in the 4000–400 cm^{-1} range. Thermogravimetric analyses were carried out on Perkin-Elmer Diamond TG/DTA Thermal Analysis instrument in a nitrogen atmosphere with a heating rate of 10 $^{\circ}Cmin^{-1}$ and a 10 mg sample. The 15–300 K magnetization measurements were carried out on a Quantum Design PPMS system. χ–T graphs were recorded under the constant magnetic field of 0.5 kOe. Magnetic data were corrected for the diamagnetic contribution of the sample holder.

2.2. Synthetic procedure

2.2.1. *Synthesis of compound $[Ni(hydeten)_2Ag(CN)_2][Ag(CN)_2].H_2O$ (**C1**)*

To ethanol (5 mL) and water (15 mL) solution of $AgNO_3$ (250 mg, 1.470 mmol) was added solid KCN (190 mg, 1,450 mmol) and clear $K[Ag(CN)_2]$ solution was formed. Then, $NiCl_2.6H_2O$ (350 mg, 1.470 mmol) was added to the solution of $K[Ag(CN)_2]$ resulting in a light blue slurry. When *hydeten* (220 mg, 1.480 mmol) was added to the obtained slurry under continuous stirring, a pink precipitate was formed within 5 minutes. The product was filtered off, washed with water and alcohol, and then dried in air. Yield: 52 %. Anal. Calc. (%) for $C_{12}H_{26}N_8O_3Ag_2Ni$: *C* 23.83, *H* 4.33, *N* 18.53, found: *C* 24.12, *H* 4.33, *N* 19.12. IR spectra (KBr disk; cm^{-1}) 3500, 3438 [υ(O–H)]; 3355, 3291, 3266 [υ(N–H)]; 2948, 2869 [υ(C–H)]; 2161, 2142 [υ(C≡N)]; 1602 [δ(N–H)]; 1064, 1029 [υ(C-O)].

2.2.2. *Synthesis of compound $[Cd_2(hydeten)_2Ag_4(CN)_8].H_2O$ (**C2**)*

Solid KCN (1.76 mmol, 0.23 g) was added to 20 mL $AgNO_3$ (1.76 mmol, 0.3 g) solution in an ethanol:water (1:1) mixture. $CdSO_4.8/3H_2O$ (1.7 mmol, 0.45 g) was slowly added to this solution and a cloudy cream mixture was appeared. Then, the suspension was added slowly to *hydeten* (1.77 mmol, 0.37 g) with stirring. The resultant clear solution was left to crystallize at room temperature, and white crystals of ***C2***, suitable for X-ray analysis, formed by slow evaporation after about a week. Yield: 41 %. Anal. Calc. (%) for $C_{16}H_{24}N_{12}O_3Ag_4Cd_2$: *C* 17.65, *H* 2.22, *N* 15.44, found: *C* 18.04, *H* 2.39, *N* 16.12. IR spectra (KBr disk cm^{-1}) 3612, 3586 [υ(O–H)]; 3442, 3355, 3280 [υ(N–H)]; 2962, 2902, 2846 [υ(C–H)]; 2150 [υ(C≡N)]; 1606 [δ(N–H)]; 1035 [υ(C-O)].

2.3. Crystallography

For the crystal structure determination, the single-crystal of ***C2*** was used for data collection on a Rigaku R-AXIS RAPID-S imaging plate diffractometer. The graphite-monochromatized Mo K_α radiation (λ=0. 71073 Å) and oscillation scan technique with $\Delta\omega$=5° for one image were used for data collection. The lattice parameters were determined by the least-squares methods on the basis of all reflections with $F^2>2\sigma(F^2)$. Integration of the intensities, correction for Lorentz and polarization effects and cell refinement was performed using CrystalClear software [33]. The structures were solved by direct methods using SHELXS-97 and refined by a full-matrix least-squares procedure using the program SHELXL-97 [34]. Hydrogens attached to carbon and nitrogen atoms were positioned geometrically and refined using a riding model. Crystal data and structure refinement parameters for ***C2*** are presented in Table 1.

Table 1. Crystal data and structure refinement of ***C2***

Empirical formula	$C_{16}H_{24}Ag_4Cd_2N_{12}O_3$
Formula weight	1088.75
Temperature [K]	293(2)
Crystal size [mm]	0.1x0.2x0.3
Crystal system	Monoclinic
Space group	$P2_1/c$
a [Å]	15.7839(2)
b [Å]	12.0002(2)
c [Å]	15.8813(4)
α = γ [°]	90.00
β [°]	96.1870(10)
V [$Å^3$]	2990.56(9)
Z	4
ρcalcd. [g/cm^3]	2.418
μ [1/mm]	4.00
F(000)	2048
Θ range [°]	2.4-26.5
Index ranges	±19, -14/15, -18/19
Reflections collected	61375
Reflections observed(>2σ)	4916
Data/restrains/parameters	4916/1/ 327
R1 (all)	0.0562

wR2	0.1078
GooF	1.102

2.4. Biological Studies

2.4.1. Preparation of microorganisms

A total of 10 microbial cultures belonging to ten bacterial species were used in this study. The cultures were grown in Mueller–Hinton Broth (Merck) for all the bacterial strains for 24 h of incubation at 36 ^{o}C.

2.4.2. Disc diffusion assay

Antibacterial tests were carried out by disc-diffusion method [35] using 100 µL of suspension containing 10^8 CFU/mL of bacteria and 10^6 CFU/mL of yeast spread on Nutrient Agar (NA) and Potato Dextrose Agar (PDA) medium, respectively. The blank discs (Oxoid = 6 mm in diameter) were impregnated with 20 µL of the each substance (105 µg/disc) and placed on the inoculated agar. Negative control (KCN) was prepared using the same solvent (water) employed to dissolve each substance. Sulbactam (30 µg) + Cefoperazona (75 µg) (105 µg/disc) was used as positive reference standard to determine the sensitivity of a strain of each bacterial species tested. The inoculated plates were incubated at 36 ^{o}C for 24 h for clinical bacterial strains. Antibacterial activity was evaluated by measuring the zone of inhibition against the test organisms.

2.4.3. Microdilution assay

The minimal inhibition concentration (MIC) values were also studied for the microorganisms, which were determined to be sensitive to the substances tested in the disc-diffusion assay. İnocula of microorganisms were prepared using 12 h broth cultures and suspensions were adjusted to 0.5 McFarland standard turbidity. Each substance dissolved in 10% dimethyl sulfoxide (DMSO) was first diluted to the highest concentration (1000 µg/mL) to be tested. Then, serial twofold dilutions were made in a concentration range from 3.9–1000 µg/mL in 10-mL sterile test tubes containing nutrient broth. A prepared suspension of the standard microorganisms was added to each dilution in a 1:1 ratio. Growth (or its lack) of microorganisms was determined visually after incubation for 24 h at 36 ^{o}C. The lowest concentration at which there was no visible growth (turbidity) was taken as the MIC. This process was also repeated for the antibiotic. MIC values of the compounds against bacterial strains were determined on the basis of a micro-well dilution method [36].

2.4.4. Test fungi

Two plant pathogenic fungi, namely *Alternaria solani*, and *Rhizoctonia solani* were obtained from a culture collection of Department of Plant Protection, Agricultural Faculty, Gaziosmanpasa University. They were maintained on potato dextrose agar (PDA) medium and then stored at 4 ºC. All the fungi were activated and then subcultured from 7 days in darkness at 25 ± 2 ºC by transferring from the stock cultures to PDA medium in Petri dishes before use.

2.4.5. Agar well diffusion bioassay

The antimicrobial test was performed according to the method of Boyanova et al. with some modification [37]. Briefly, A 20 mL of PDA medium was poured into a 9-cm diameter sterile Petri dish before solidification. Discs (5-mm diameter) of the mycelial plugs from the edge of the cultured fungal colony were cut and placed mycelial surface down on the one side of the dishes and the wells (5 mm holes) were produced in the agar with sterile cork borer at 30 mm apart from mycelial discs of the fungus on opposite sides of Petri dishes. The ***C1*** and ***C2*** were diluted with sterile distilled water to the final concentrations of 2.5, 5, 7.5, 10, 12.5, 15, and 20 µg/mL. Of these, 20 µL of the diluted samples were pipetted into the well. All plates were then incubated in the dark at 25 ± 2 ºC for 7 days. Reading the results was carried out by measuring the diameters of the zones of inhibition and clear growth (in mm). Three replicates were used for each treatment. Sterile distilled water was used as the control. The diameter of the inhibition zone was measured when the hyphae of the control extended to whell in where 20 µl sterile distilled water was loaded with control plates. The rates of mycelial growth inhibition (GI%) were calculated by the following formula: GI% = dc-dt/dc*100 Where dc is mean colony diameter of control sets and dt is the mean colony diameter of treatment sets [38]. Each test was run in triplicate.

2.4.6. Statistical analysis

Analysis of variance (ANOVA) was used to determine the effects of the chemicals on mycelial growth inhibition of fungi. Statistical analysis was performed with SAS (version 9.1.3) statistic softwares. Data that did not show variance homogeneity were analysed by the non-parametric Kruskal-Wallis test. Inhibition zone data were analyzed using POLO-PC Probit [39] to estimate lethal concentration 50, and 90 values (LC50, and 90) and the regression line slope.

2.5. Anticancer Studies

2.5.1. Cell Culture

C6 (rat brain tumor cells), HT29 (human colon cancer cells) and HeLa (human cervical cancer cells) cell lines were maintained in Dulbecco's modified eagle's medium (DMEM, Sigma), supplemented with 10 % (v/v) fetal bovine serum (Sigma, Germany) and PenStrep solution (Sigma, Germany). At confluence, cells were detached from the flasks using 4 mL of trypsin–EDTA (Sigma, Germany), centrifuged and cell pellet resuspended with 4mL supplemented DMEM.

2.5.2. BrdU Cell Proliferation Assay (BCPA)

Cell suspension containing $3x10^3$ cells in 100 µL was pipeted into wells of 96-well cell culture plates (COSTAR, Corning, USA). Test compounds (***C1***, ***C2***) and control compound (5 flourourasil, *5FU*) was dissolved in sterile DMSO. DMSO amount was adjusted to

0.5%. The cells were treated with ***C1*** and ***C2*** and 5FU at final concentrations of 5, 10, 20, 30, 40, 50, 75, and 100 µg/mL. Cell controls and solvent controls were treated with supplemented DMEM and sterile DMSO respectively. The final volume of the wells was adjusted to 200 µL by supplemented DMEM. The cells then were incubated at 37°C with 5 % CO_2 for overnight. The antiproliferative activity of the compounds was determined using BrdU Cell proliferation ELISA Kit (Roche, USA), a calorimetric immunoassay based on BrdU incorporation into the cellular DNA, according to manufacturer's protocol. Briefly, cells were exposed to BrdU labeling reagent for 4 h followed by fixation in FixDenat solution for 30 min at room temperature. Then, cells were cultured with 1:100 diluted anti-BrdU-POD for 1.30 h at room temperature, substrate solution was added to each well and BrdU incorporation was measured at 450-650 nm using a microplate reader (Rayto, China). Each experiment was repeated at least three times for each cell line.

2.5.3. *Calculation of % inhibition and IC_{50}*

In BCPA assay results were reported as percent inhibition of test and control substances. The percent inhibition was calculated according to the formula: % inhabitations [1-(Absorbance of Treatments/ Absorbance of DMSO) × 100]. The half maximal inhibitory concentration (IC_{50}) of the test and control compounds was calculated using XLfit5 software (IDBS) and expressed in µg/mL at 95% confidence intervals.

2.5.4. *Lactate Dehydrogenase (LDH) Cytotoxicity Assay*

Cytotoxicity of ***C1*** and ***C2*** on C6, HT29, HeLa cells was determined through the calorimetric LDH Cytotoxicity Detection Kit (Roche, USA) based on the measurement of LDH activity released from the cytosol of damaged cells into the supernatant according to manufacturer's instructions. $3x10^4$ cells in 100 µL were seeded into 96-well microtiter plates as triplicates and treated with IC50 concentrations of ***C1*** and ***C2*** as described above at 37°C with 5% CO_2 for overnight. LDH activity was determined by measuring absorbance at 492-630 nm using a microplate reader.

2.5.5. *Analysis of DNA laddering*

DNA laddering effect of the test compounds was measured according to the method of Gong [40] with some modifications. Briefly, $7.5x10^5$ cells were seeded into 25 cm^2 culture flasks, and treated with IC_{50} concentrations of ***C1*** and ***C2*** at 37°C with 5 % CO_2 for overnight. Treated cells were harvested using a sterile plastic scraper, transferred to a 15 mL sterile Falcon tube, washed with 1 mL sterile DPBS, and pelleted by spinning at 1500xg for 5 min. The cell pellet resuspended with 200 µL ice cold DPBS by gently pipeting, fixed with 5 mL ice cold 70% ethanol, vortexed shortly and incubated at -20°C for 24 hours. The cells were centrifuged at 1500xg for 5 min, the supernatant was removed and the remaining ethanol removed by air drying. The cell pellet was resuspended in 50 µL phosphate-citrate buffer (consisting of 192 parts of 0.2 M Na_2HPO_4 and 8 parts of 0.1 M citric acid, pH 7.8), incubated at 37°C for 30 min in a shaker incubator, and centrifuged at 1500xg for 5 min. A 40 µL of supernatant was transferred to a 1.5 mL microsantrifuge tube, mixed with 5 µL Tween20 solution (0.25 % in ddH_2O) and 5 µL RNase A solution and incubated at 37°C for 30 min in a shaker incubator. Then, 5 µL proteinase K was added to each tube and incubated at 37°C for 10 min. Finally, the entire content of the microcentrifuge tube was mixed with 4 µL of 6X loading buffer, loaded to 1.5% agarose gel containing 0.5 µg/mL ethidium bromide and electrophoresed at 200 mA for 40 min. DNA laddering in the gels was visualized using gel documentation system (UVP, England).

2.5.6. *Terminal deoxynucleotydil transferase dUTP nick end labeling (TUNEL) assay*

For *in vitro* detection of apoptosis at the single-cell level was assessed using TUNEL assay (Roche, Germany) and was performed according to the manufacturer's protocol. HT29 cell lines (30.000 cells/well) were placed in poly-L-lysine covered chamber slide. The cells were treated with IC_{50} concentration of ***C1*** and ***C2*** left for 24 hours incubation. There were two controls for this assay, one was positive control that had DNase-1 treatment and the other was negative control that had no terminal deoxynucleotidyl transferase (TdT). When the incubation time was over, the chamber was removed from slide and washing with DPBS to get rid of the medium and unattached cells. All the incubation and washing steps were done in a plastic jar. Slides were gently washed with DPBS and for fixation 4% paraformaldehyde in DPBS, pH 7.4, were prepared freshly and added to slides for 60 min at room temperature. Following incubation, the slides were washed twice with DPBS. The cells were blocking with freshly prepared 3% H_2O_2 in methanol for 10 min at room temperature. Following incubation, the slides were washed twice with DPBS. The cells were permeabilized by prechilled 0.1% Triton X-100 and 0.1% sodium citrate in water, freshly prepared, and incubated for 2 minutes on ice. All the slides were washed with DPBS twice for 5 minutes each. At this point in order to prepare a DNase I enzyme treated positive control, 100 µl of DNase-1 Buffer was added to slide and incubated at room temperature for 10 minutes. Fixative cells were transferred into TUNEL reaction mixture (50 µL/section) containing a TdT and fluorescein-dUTP. Intracellular DNA fragments were then labeled by exposing the cells to TUNEL reaction mixture for 1 h at 37˚C, in a humidified atmosphere and protected from light. After washing with DPBS twice cells positive for apoptosis showed a green fluorescent signal and were visualized by a Leica fluorescent microscope (Leica DMIL LED fluo, Germany).

2.5.7. *Cell migration assay*

The migration inhibitory capability of the compounds was measured using the cell migration assay. Briefly, a culture insert (ibidi GmbH, Germany) which consists of two reservoirs separated by a 500 µm thick wall, was placed on a 35-mm petridish, and an equal number of HeLa cells (3.5×10^4 HeLa cells in 70 µL DMEM medium) were seeded into the two reservoirs of the same insert and allowed to grow to 90–95% confluence, in order to generate a 500 µm gap between two cell populations. Subsequent to cell growth, the insert was gently removed and 2 ml of cell culture medium was added and

treated with IC_{50} concentrations of ***C1*** and ***C2*** for overnight at 37°C with 5% CO_2. The closure of the gap by the cells was photographed 0, 1 and 2 days after incubation by using a phase contrast inverted microscope (Leica DMIL, Germany).

2.5.8. DNA topoisomerase I inhibition assay

DNA topoisomerase I inhibitory activities of the compounds in cell-free systems were evaluated by using topoisomerase I assay kit (TopoGen, USA). The principle of the assay is to measure the conversion of supercoiled pHOT1 plasmid DNA to its relaxed form in the presence of DNA topoisomerase I alone and with test compounds. The supercoiled substrate (pHOT1 plasmid DNA) and its relaxed product can easily be distinguished in agarose gel because the relaxed isomers migrate more slowly than the supercoiled isomer. In brief, 20 µL of reaction mixture containing 1 µL plasmid pHOT1 DNA in relaxation buffer was incubated with 2U recombinant human topoisomerase I in the presence of IC_{50} concentrations of ***C1, C2*** or camptothecin as positive control. The reactions were carried out at 37˚C for 30 min and then terminated by the addition of stop solution. After the termination, the sample was analyzed using a 1% agarose gel at 4 V/cm for 60 min. After electrophoresis DNA bands were stained with ethidium bromide (1 mg/ml) solution and photographed through a gel imaging system (UVP BioSpectrum, Germany).

III. Results and Discussion

3.1. Infrared Spectroscopy (*IR*)

The formation of a cyanido bridge in a polymeric complex was shown by the stretching vibration region of the cyanido ligand in *FT-IR* spectra. The cyanido group as a ligand can be bound by various modes. There are two binding modes which most commonly occur in *1D* cyano complexes; the cyanido group can act as a terminal ligand with the carbon donor atom or bond through both carbon and nitrogen donor atoms and act as a μ_2-bridging ligand [41]. Also, the use of different *N*-donor ligands (e.g. *hydeten*) led to various types of structures and different function of the cyanido groups (e.g. terminal or bridging), which is reflected by the ν(CN) stretching vibration positions in the *IR* spectra of ***C1*** and ***C2***.

The formation of dicyanidoargentates is confirmed by the strong ν(CN) stretching bands. The position of the ν(CN) stretching vibration is an important tool for distinguishing between terminal and bridging character of the cyanido group. This band is observed at 2080 cm^{-1} in free CN^- (aqueous solution) [42]. As a consequence of a cyanido group coordination, ν(CN) band is shifted towards higher frequencies. While the ν(CN) position is at 2140 cm^{-1} in the solid $K[Ag(CN)_2]$, this band is shifted to 2164 cm^{-1} by formation of a cyanido bridge [43].

The single cyanido peak at 2150 cm^{-1} suggests that all cyanido groups act as bridged ligands in the ***C2***. Two peaks observed at 2142 and 2161 cm^{-1} in the ***C1*** point out the presence of both terminal and bridging cyanido groups. The lattice environment of water molecules in the complexes structure determines the position of the infrared peaks of water and whether they are singlet or multiplet [44] .The ν(OH) peaks of ***C2*** are observed at 3612 and 3586 cm^{-1}, while the ν(OH) peaks for ***C1*** are observed at 3500 and 3438 cm^{-1}.

-NH and $-NH_2$ stretching vibration peaks of the neutral ligand for ***C1*** and ***C2*** are observed between 3265 cm^{-1} and 3355 cm^{-1}, as expected. It can be seen from the *IR* spectra of ***C1*** and ***C2*** that -CH stretching peaks belonging to *hydeten* ligand appear in the 2962-2846 cm^{-1} range. δ(N-H), $\delta(CH_2)$, ν(C-N), ν(C-O) and ν(M-C) vibration peaks in the fingerprint region are the other peaks indicating existence of *hydeten* ligand.

3.2. Structure Description

The single crystal x-ray analysis of ***C1*** was not determined because suitable crystals had not been obtained. Using elemental, IR, thermal and magnetic measurements, it is estimated that the molecular structure of ***C1*** have $[Ni(hydeten)_2Ag(CN)_2]$ $[Ag(CN)_2].H_2O$ closed formula.

*3.2.1. $[Cd_2(hydeten)_2Ag_4(CN)_8].H_2O$ (**C2**)*

As shown in the thermal ellipsoid plots of ***C2*** (Figure1*a*), the thermal parameters of O3 atom in $O(3)H_2$ are too big. Therefore detection of the hydrogen peaks of the $O(3)H_2$ molecule is impossible in the difference fuorier analysis.

The results of the X-ray analysis showed that ***C2*** exhibit asymmetric unit structure formed of sixnuclear $-(CN)_2-Cd(hydeten)-NC-Ag_2-CN-Cd(hydeten)(NC-Ag-CN)_2-(NC)-$ molecules (Figure1*a*). As far as we know, a structure made up of these type chains has not been described. In ***C2***, Ag^I is coordinated by two cyanido *C*-, while the coordination sphere of Cd^{II} is composed of one *hydeten N*- and four cyanido *N*-. Thus, a *1D* polymeric chain is obtained, in which Cd^{II} and Ag^I ions are linked by *CN* groups and *3D* structure forms via $[Ag(CN)_2]^-$ bridges. In the solid state, both $[Cd(hydeten)]^{2+}$ and $[Ag(CN)_2]^-$ groups are not located on the symmetry plane; however, the Cd^{II} and Ag^I ions are located on inversion centers. Hence both ions are centrosymmetric (Figure 1*b*).

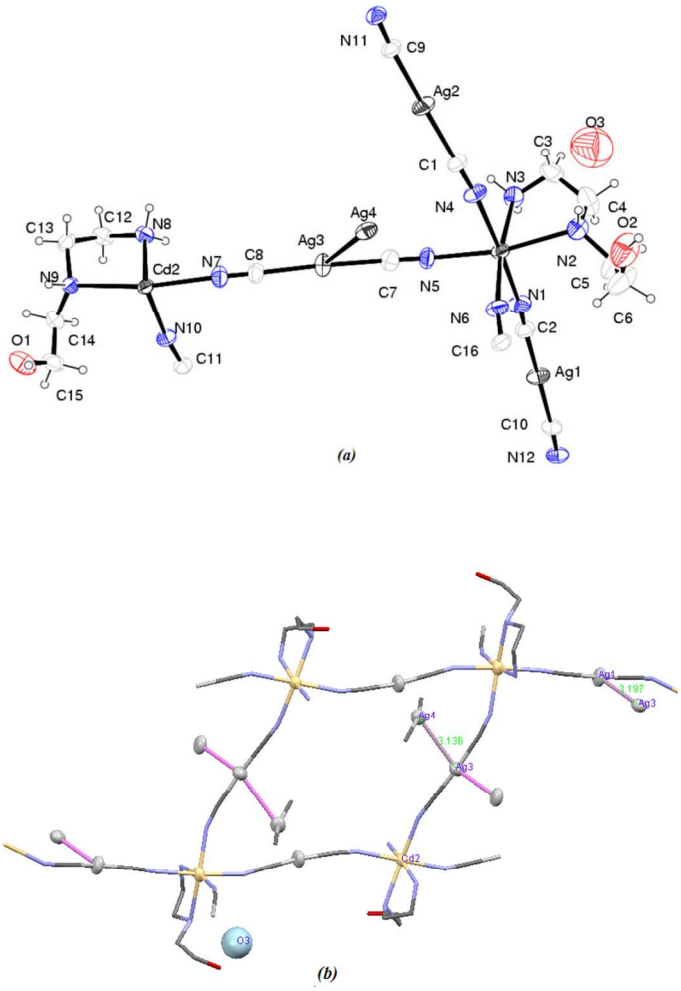

Figure 1. (***a***) The view of ***C2*** showing the crystallographic independent part and the coordination environment of metal ions. The thermal ellipsoids are drawn at 50% probability. (***b***) Mercury drawing of the centrosymmetric structure of the ***C2***

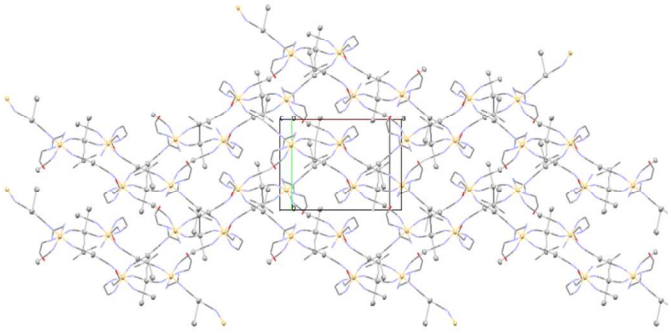

Figure 2. 6,4 ladder-type polymeric chain structure formed by $Ag_6(CN)_{12}^{6-}$ and $Cd_4(hydeten)_4^{8+}$ units.

In ***C2***, *hydeten* and cyanido ligands result in not only a centrosymmetric unit but also structural regulation of the *3D* 6,4 ladder-type polymeric chains (Figure 2). According to the array of cationic and anionic units, chain structure of cyanido bridged complexes can be classified. Chains are named by using the number of links connecting the given block to its neighbor blocks within *1D* system [41]. Based on this information, the chain structure of ***C2*** can be coded as a 6,4 ladder-type chain because both $Ag_6(CN)_{12}^{6-}$ and $Cd_4(hydeten)_4^{8+}$ units formed one leg of the ladder are surrounded by units adjacent to each other as in Scheme 1 (A for anionic unit and C for cationic unit). As a result, new ladder type chains occurred with such an arrangement of these anions and cations (Figure 3).

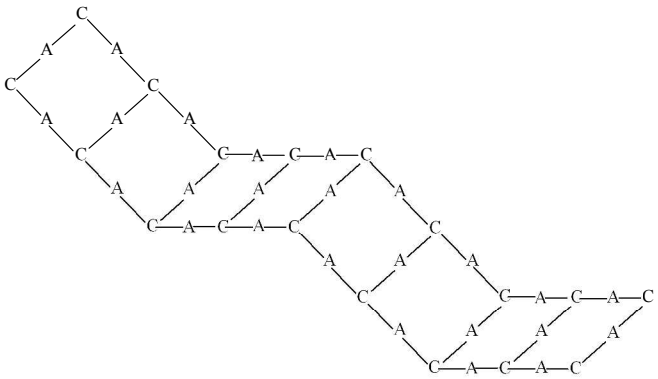

Scheme 1. Array of cationic and anionic units in a *6,4-ladder* of ***C2***

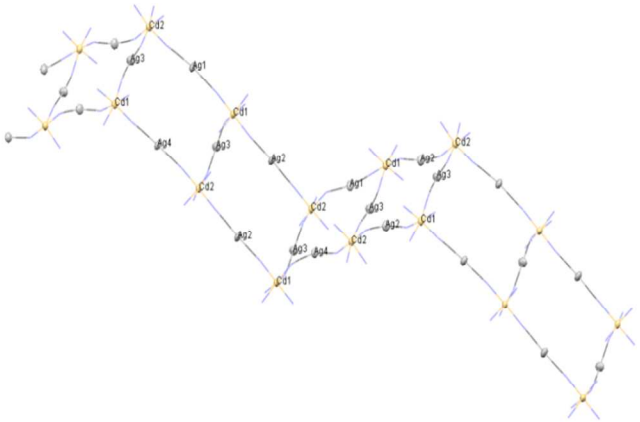

Figure 3. 6,4 ladder-type polymeric chain structure of ***C2***. Non-coordinated atoms and argentophilic interactions are omitted.

The octahedral Cd coordination environment comprises of two -*N* atoms from neutral amine ligands and two -*N* atoms from cyanido ligands located in the equatorial plane and two cyanido -*N* donors at the axial sites. Cd2-N11^{vii} and Cd2-N12^{vi} (vi: $-x+2, y-1/2, -z-1/2$; vii: $-x+1, -y+1, -z$) bond lengths in the title complex are in accordance with Cd-N3 and Cd-N4 distances as in similar Cd^{II} complex.[27] Cd-N2 bond distance is the longest one in the cadmium coordination environment (Table 2). This may be a consequence of the steric bulkiness of the free ethanolic branch of *hydeten* ligand. These distances are found to be similar to those of previously reported heteronuclear $[Cd(hydeten)_2Ni(CN)_4]$ [27],

$[Cd(hydeten)_2Pt(CN)_4]$, $[Zn(hydeten)_2Pt(CN)_4]$ [31] and $[Zn(hydeten)_2Pd(CN)_4]$, $[Cd(hydeten)_2Pd(CN)_4]$ [45] complexes reported by our group.

Table 2. Selected bond lengths [Å] for ***C2***

Bond Lengths			
Ag1-C2	2.058(8)	N2-Cd1	2.431(7)
Ag1-C10	2.060(8)	N3-Cd1	2.306(6)
Ag2-C1	2.086(7)	N4-Cd1	2.372(6)
Ag2-C9	2.068(7)	N5-Cd1	2.341(7)
Ag3-C7	2.080(9)	N6-Cd1	2.275(6)
Ag3-C8	2.071(8)	N7-Cd2	2.300(7)
Ag4-C16^{ii}	2.062(7)	N8-Cd2	2.345(6)
Ag4-C11^{iii}	2.073 (7)	N9-Cd2	2.386(6)
Ag1^{i}-Ag3	3.1964(10)	N10-Cd2	2.363(6)
Ag3-Ag4	3.1365(9)	N11^{vii}-Cd2	2.381(5)
N1-Cd1	2.342(6)	N12^{vi}-Cd2	2.316(6)

All the N–Cd–N bond angles deviate significantly from the 90° and 180°, which is presumably the result of the steric constraints arising from the shape of the ligands. The angles between Cd(II) atoms and *hydeten* ligands are 75.1(2)° and 76.3(2)°, respectively, which are in agreement with previously reported values for other *hydeten* complexes [28,31,46] The C1–N4–Cd1 and C11–N10–Cd2 bond angles are 163.6(7)° and 158.2(6)°, respectively, which result in the formation of a one-dimensional zig-zag chain, while the Ag2–C1–N4 and angles Ag4–C11–N10 [178.2(8)° and 178.7(7)°] is essentially linear (Table 3).

Ag^I is surrounded by two cyanido ligands which form bridges between Ag^I and Cd^{II} atoms in *trans* fashion. While Ag-C-N angles are almost linear with a small deviation, Cd-C-N angles can vary over a wide interval from almost 120 to 180° [27] C-N bond lengths of the bridging cyanido groups are slightly longer than that of terminal cyanido groups (Table 3).

Remarkably, Ag metal centers assemble through ligand-unsupported d^{10}–d^{10} interactions. The Ag–Ag distances of the trimeric fragments, which range from 3.1965(9) to 3.1365(9) Å, are below the sum of the van der Walls radii of two silver atoms (3.44 Å) [47] The trimeric Ag1-Ag3-Ag4 chain is a bit curved. The short Ag…Ag argentophilic interactions (Ag1…Ag3=3.1964(10) and Ag3….Ag4= 3.1365(9) Å) are a characteristic of the silver compounds [48] and they contribute to the packing forces of the crystal structure (Figure 3).

Table 3. Selected bond angles [°] for ***C2***

Bond Angles			
Ag1-C2-N1	176.4(8)	N1-Cd1-N2	93.1(3)
Ag1-C10-N12	176.7(8)	N1-Cd1-N4	176.2(3)
Ag2-C1-N4	178.2(8)	N1-Cd1-N5	90.5(3)
Ag2-C9-N11	175.1(7)	N3-Cd1-N1	90.8(3)
Ag3-C7-N5	172.1(8)	N3-Cd1-N2	75.0(2)
Ag3-C8-N7	178.9(8)	N3-Cd1-N4	88.1(3)
Ag4^{v}-C11-N10	178.7(7)	N3-Cd1-N5	93.5(3)
Ag4^{ii}-C16-N6	172.2(7)	N4-Cd1-N2	90.1(3)
C2-Ag1-C10	171.3(3)	N5-Cd1-N2	168.0(2)
C11^{iii}-Ag4-C16^{ii}	164.0(3)	N5-Cd1-N4	85.9(3)
C7-Ag3-C8	174.6(3)	N6-Cd1-N1	87.1(3)
C1-Ag2-C9	173.1(3)	N6-Cd1-N2	97.2(3)
Ag3^{i}-Ag1-C2	103.6(2)	N6-Cd1-N3	171.8(3)
Ag3^{i}-Ag1-C10	85.0(2)	N6-Cd1-N4	94.6(2)
Ag3-Ag4-C11^{iii}	82.2(2)	N6-Cd1-N5	94.4(3)
Ag3-Ag4-C16^{ii}	100.1(2)	N7-Cd2-N8	94.7(2)
Ag4-Ag3-C7	69.0(2)	N7-Cd2-N9	170.6(2)
Ag4-Ag3-C8	107.2(2)	N7-Cd2-N10	88.0(2)
Ag1^{i}-Ag3-C7	79.0(2)	N7-Cd2-N11^{vii}	92.6(2)
Ag1^{i}-Ag3-C8	106.4(2)	N7-Cd2-N12^{vi}	94.0(3)
Ag1^{i}-Ag3-Ag4	126.28(3)	N8-Cd2-N9	76.3(2)
C2-N1-Cd1	173.7(8)	N8-Cd2-N10	89.1(2)
C4-N2 -Cd1	105.4(6)	N8-Cd2-N11^{vii}	92.4(2)
C5-N2-Cd1	123.4(7)	N10-Cd2-N9	94.6(2)
C3-N3-Cd1	109. 7(5)	N10-Cd2-N11^{vii}	178.3(2)
C1-N4-Cd1	163.6(7)	N11-Cd2-N9	85.1(2)
C7-N5-Cd1	162.5(7)	N12^{vi}-Cd2-N8	169.6(2)
C16-N6-Cd1	163.2(7)	N12^{vi}-Cd2-N9	95.2(2)
C11-N10-Cd2	158.2(6)	N12^{vi}-Cd2-N10	85.5(2)
C10-N12-Cd2^{iv}	155.7(7)	N12^{vi}-Cd2-N11^{vii}	92.9(2)

i) $-x+2, -y+2, -z$; (ii) $-x+2, -y+1, -z$; (iii) $x, -y+3/2, z+1/2$; (iv) $-x+2, y+1/2, -z-1/2$; (v) $x, -y+3/2, z-1/2$; (vi) $-x+2, y-1/2, -z-1/2$; (vii) $-x+1, -y+1, -z$.

All of the Ag^I ions in the trimeric chains are located on the same least square plan. As far as we are aware, these linear oligocyanidoargentate anions $[Ag(CN)_2]_n^{n-}$ (n = 3 or 5) assembled via the d^{10}–d^{10} interaction are rarely observed [49] (Figure 4). ***C2*** represents the first example of oligocyanidoargentate anion $[Ag(CN)_2]_n^{n-}$ (n = 3) assembled through ligand-unsupported d^{10}–d^{10} interactions in the solid state.

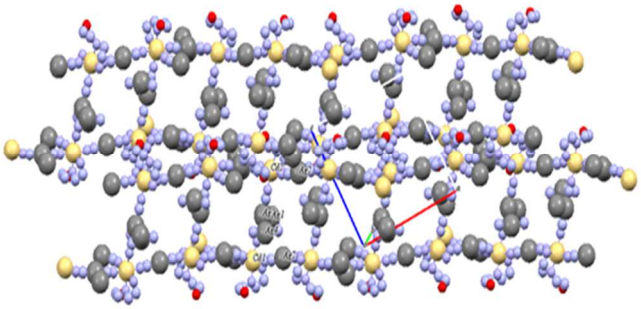

Figure 4. A polymeric structure consisting of linear oligocyanidoargentate anions $[Ag(CN)_2]_n^{n-}$ assembled via the d^{10}–d^{10} interaction.

All amine hydrogens are involved in hydrogen bonding (*HB*) and a three dimensional structure is formed by the aid of *HB*s listed in Table 4.

Table 4. Selected intermolecular distances [Å] and angles [°] of ***C2***

D–H···A	*D–H*	*H···A*	*D···A*	*D–H···A*
O(1)-H(1) ···N(12)^{i}	0.76	2.54	3.218(4)	149
O(2)-H(2) ···N(5)^{ii}	1.00	2.62	3.435(4)	137
N(2)-H(2A) ···O(2)	0.91	2.51	2.906(5)	106
N(3)-H(3B) ···O(2)^{iii}	0.90	2.28	3.078(4)	148
N(8)-H(8A) ···O(1)^{iv}	0.90	2.19	3.024(5)	153
N(9)-H(9A) ···O(1)	1.02	2.51	2.905(4)	102

3.3. Thermal Analyses

Thermal stabilities and decomposition behaviors of ***C1*** and ***C2*** are studied by *TG-DTA* in the flowing atmosphere of N_2. The general way of the thermal decomposition of cyanido complexes is characterized by leaving of *N*-donor ligands and then decomposition of all cyanido groups in one step [46,49-52]. Thermal decompositions of ***C1*** and ***C2*** are multi-stage processes. Thermal analysis data for ***C1*** and ***C2*** are represented in Table 5.

(Insert Table 5 here)

First process in the thermal decomposition of ***C1*** is dehydration and the release of two *hydeten* molecules in the 194-532 °C temperature range with an endothermic process (found 37.82 % calc. 37.39 %). The observed total weight loss of 16.89 % corresponds to the liberation of all four cyanido molecules in the 532-828 °C temperature range (calc. 17.20 %).

In the 71–1195 °C temperature range, five processes are observed for ***C2***. In the 71-367 °C temperature range, an observed weight loss of 19.90 % corresponds to the liberation of two *hydeten* molecules (calc. 19.42%). The release of eight cyanido molecules and two Cd atoms, the boiling points of which are 985 °C, observed with the total weight loss of 40.36 % (calc. 39.73 %). The most probable thermal decomposition scheme of ***C1*** and ***C2*** is given below:

$$[Ni(hydeten)_2Ag_2(CN)_4].H_2O \xrightarrow[-H_2O,\ -2\ hydeten]{35\text{-}532^oC} [NiAg_2(CN)_4]$$
C1

$$[NiAg_2(CN)_4] \xrightarrow[-4\ CN]{532\text{-}825^oC} NiAg_2$$

$$[Cd_2(hydeten)_2Ag_4(CN)_8].H_2O \xrightarrow[-H_2O,\ -2\ hydeten]{35\text{-}367^oC} [Cd_2Ag_4(CN)_8]$$
C2

$$[Cd_2Ag_4(CN)_8] \xrightarrow[-8\ CN,\ -2\ Cd]{367\text{-}1195^oC} 4Ag$$

3.4. Magnetic Property

The magnetic susceptibility of ***C1*** was obtained in the temperature range of 10–300 K. The temperature dependence of the molar magnetic susceptibility (χ_m) and χ_mT is shown in Figure 5 for ***C1***. The temperature dependence of χ_m was fitted by relation of $\alpha+C/(T-\theta)$ where α is temperature independent susceptibility [53]. Determined fitting results: C= 1.21857±0.00025 emuK/mol.O, α=0.00033± 0.000002 emu/mol.Oe and θ = -0.484 ± 0.002 K. Here, there is temperature independent paramagnetism (α). This can occur when the ground state couples with exciting states due to the orbital moments of *d* electrons or when there are itinerant (conducting) electrons. The effective magnetic moment for ***C1***, *μeff*, was calculated to be 3.125 using the relation $\mu_{eff} = 2.83(C)^{1/2}$ in Bohr magneton (μ_B). The values of *μeff* for this ***C1*** seem above the spin only value due to mixing of some spin-orbital angular momentum from excited states via spin- orbit coupling [54].

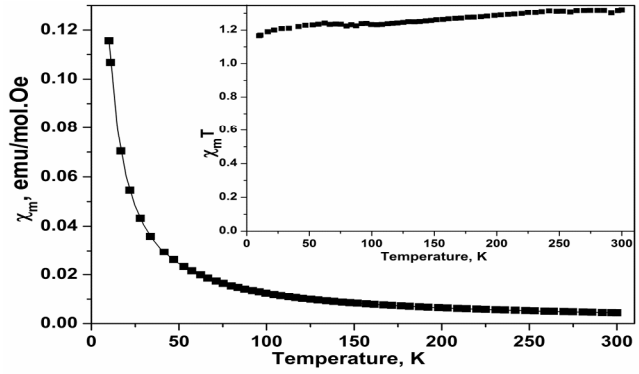

Figure 5. The temperature dependence of the molar magnetic susceptibility χ_m for ***C1***.The solid line represents a fit by the Curie–Weiss law. Inset: The temperature dependence of χ_m.

Below 10K, for both ***C1*** there might be a very small antiferromagnetic interaction in the structure, as seen from the knee

down in the inset of Figure 5. This magnetic interaction might be between and within the chains through CN^- bridges and *HB*s.

3.5. Antibacterial Activity

The newly synthesized ***C1*** and ***C2*** underwent general antibacterial screening. A yeast (*Candida utilis* KUEN 1031), four gram-positive bacteria (*Staphylococcus aureus* ATCC 29213, *Bacillus subtilis* ATCC 6633, *Bacillus cereus* DSM 4312, *Streptococcus Pyogenes* ATCC 176), and five gram-negative bacteria (*Escherichia coli* 111, *Escherichia aerogenes* 2924, *Salmonella gallinarum*, *Pseudomonas aeruginosa* ATCC 27859, and *Salmonella enteridis* ATCC 13076) were selected to evaluate the effectiveness of the test complexes (***C1*** and ***C2***).

C1 and ***C2*** were screened for their antibacterial activity against one yeast bacteria viz., (*Candida utilis* KUEN 1031), four gram positive bacteria viz., *Staphylococcus pureus* ATCC 29213, *Bacillus subtilis* ATCC 6633, *Bacillus cereus* DSM 4312, *Streptococcus pyogenez* ATCC 176, and five gram negative bacteria viz., *Escherichia coli* 111, *Enterobacter aerogenes* 2924, *Salmonella gallinarum, Pseudomonas aeruginosa* ATCC 9027, *Salmonella enteridis* ATCC 13076, by using disc-diffusion method. A reference standard drug SCF [Sulbactam (30 µg) + Cefoperazona (75 µg)] and KCN were used as positive and negative control, respectively. The experiments were performed in triplicate in order to minimize the errors. A zone of inhibition produced by each compound was measured in mm. The results of antibacterial studies were given in Table 6.

Table 6. Antimicrobial activity of ***C1*** and ***C2*** (105 µg/disc) against the bacterial strains and Candida sp. isolates using the disc diffusion method

Microorganisms	Compounds and inhibition zones (mm)			
	SCF	**KCN**	***C1***	***C2***
Gram-positive bacteria				
*S. aureus*ATCC29213	29	NE	30	26
*B. subtilis*ATCC6633	19	NE	26	27
B. cereus DSM 4312	23	NE	35	30
*St. pyogenez*ATCC176	18	NE	26	13
Gram-negative bacteria				
E. coli 111	20	NE	29	23
E. aerogenes 2924	26	NE	29	24
S. gallinarum	36	NE	47	36
*P. aeruginosa*ATCC9027	25	NE	45	28
*S. enteridis*ATCC13076	19	NE	29	28
Yeasts				
*C. utilis*KUEN1031	19	NE	23	19

SCF: [Sulbactam (30 µg)+cefoperazona (75 µg)] = positive control
KCN: Potassium cyanide = negative control: -: Inactive
NE: No effect (There is no inhibition zone)

The screening results revealed that ***C1*** and ***C2*** showed remarkable antibacterial activity. In particular, ***C1*** was more active than the positive control (SCF) for all of the bacteria. A comparison of the compounds' activity with that of standard antibiotic SCF is effectively presented in Table 6.

For *S. aureus* and *E. aerogenes 2924*, the data in Table 6 exhibits ***C1*** > SCF > ***C2*** > KCN sequence of antibacterial activity. The value of 30 mm makes us clear that the antibacterial activity of ***C1*** is the strongest. The thickness of the restrain ring bacterial against *B. subtilis* is kept in the order of ***C2*** (27 mm) > ***C1*** (26 mm) > SCF (19 mm) > KCN (0 mm). The sequence indicates that the antibacterial activity of ***C2*** is the highest, value of inhibition zone of which reaches 27 mm. Relative to controlled group SCF and KCN, two compounds still have stronger antibacterial activities against *B. subtilis*. As shown in the results of *B. cereus*, *P.* aeruginosa and *S. gallinarum*, the thickness of the inhibition zones are in the following order, respectively: ***C1*** (35 mm) > ***C2*** (30 mm) > SCF (23 mm) > KCN (0 mm), ***C1*** (45 mm) > ***C2*** (28 mm) > SCF (25 mm) > KCN (0 mm) and ***C1*** (47 mm) > **C2** (36 mm) = SCF (36 mm) > KCN (0 mm). These sequences reveal that the ***C1*** has the strongest antibacterial activity due to its inhibition zone of ΔR of 35, 45 and 47 mm, which is much bigger than others.

C1 and ***C2*** were subjected to MIC (minimum inhibitory concentrations) studies and the results are given in Table 7. Sulbactam (30 µg) + Cefoperazona (75 µg) (105 µg/disc) was chosen as positive control. SCF is a broad spectrum antibiotic. MIC values were determined by serial microdilution technique in Mueller–Hinton Broth for antibacterial assay.

Table 7. Minimum-inhibitory concentrations (MIC, in µg /ml) of ***C1*** and ***C2***

Microorganisms	Antibiotics MIC (µg /ml)			
	KCN	***C1***	***C2***	**SCF**
Gram-positive bacteria				
*S. aureus*ATCC29213	NE	62.50	62.50	125
*B. subtilis*ATCC6633	NE	62.50	31.25	500
B. cereus DSM 4312	NE	62.50	62.50	500
*St. Pyogenez*ATCC176	NE	125	62.50	500
Gram-negative bacteria				
E. coli 111	NE	15.62	31.25	250
*P. aeruginosa*ATCC9027	NE	62.50	62.50	1000
E. Aerogenes 2924	NE	31.25	31.25	62.50
S. Gallinarum	NE	31.25	15.62	62.50
*S. enteridis*ATCC13076	NE	125	15.62	1000

Yeast				
*C. utilis*KUEN1031	NE	62.50	125	500

SCF: [Sulbactam (30 µg)+cefoperazona (75 µg)] = positive control
KCN: Potassium cyanide = negative control
NE: No effect

As seen in the Table 7, both complexes showed higher activity (MIC: 31.25, 62.5, 62.5, 62.5 µg/mL) than the positive control against *E. Aerogenes, S. aureus*, *B. cereus* and *P. aeruginosa* (MIC: 62.50, 250, 500 and 1000 µg/mL, respectively).

While ***C1*** (MIC: 15.62 and 62.5 µg/mL, respectively) exhibited better activity than ***C2*** (MIC: 31.25 and 125 µg/mL, respectively) for *E. coli* and *C. utilis* bacteria, both complexes demonstrated higher activity than the positive control (MIC: 250 and 500 µg/mL, respectively). On the other hand, ***C2*** (MIC: 31.25, 62.5, 15.62 and 15.62 µg/mL, respectively) showed better activity than ***C1*** (MIC: 62.5, 125, 31.25 and 125 µg/mL, respectively) for *B. subtilis, St. Pyogenez, S. Gallinarum* and *S. enteridis* bacteria. For same bacteria, both complexes exhibited better activity than the positive control (MIC: 500, 500, 62.50 and 1000 µg/mL, respectively). Among gram-positive bacteria, ***C2*** (MIC: 31.25 µg/mL) had the best activity for *B. subtilis*. As for gram-negative bacteria, the best bacterial inhibitor was ***C1*** for *E. coli* and ***C2*** for *S. enteridis*. MIC values were studied for the same bacterial strains in the disc-diffusion assay and are given in Table 7.

3.6. Antifungal Activity

3.6.1. Antifungal activity by Agar well diffusion bioassay

Both compounds tested showed varied degrees of inhibition over control in the mycelial growth of the pathogens *A. solani* and *R. solani* at different concentrations. All the results obtained from seven different concentrations were interpreted in terms of their mean value (Table 8). The maximum mycelial growth inhibition of *A. solani* was obtained in ***C1*** with 88.38% at 20µg/mL concentration. This was followed by ***C2*** with 83.27% of the same concentration. Mycelial growth inhibition of *R. solani* was similar in both chemicals with 75.95% and 75.12% at at 20 µg/mL respectively. The inhibitory action of ***C1*** and ***C2*** on mycelial growth of the fungi increased with increase in concentrations (Table 8).

Table 8. Anti-fungal activities of chemicals against *Alternaria solani* and *Rhizoctonia solani* after 7 day

Dosage (µg/mL)	*Alternaria solani* (Growth inhibition %)*		*Rhizoctonia solani* (Growth inhibition %)*	
	C1	***C2***	***C1***	***C2***
20.0	88.38^{a}	83.27^{a}	75.95^{a}	75.12^{a}
15.0	75.37^{b}	77.20^{a}	74.27^{ab}	73.28^{a}
12.5	69.10^{b}	75.86^{a}	68.15^{b}	55.10^{b}
10.0	46.00^{c}	64.88^{b}	40.95^{c}	44.22^{c}
7.5	34.59^{d}	58.67^{b}	13.59^{d}	43.80^{c}
5.0	0.73^{e}	58.23^{b}	0.00^{e}	25.21^{d}
2.5	0.00^{e}	32.97^{c}	0.00^{e}	0.00^{e}
Control (water)	0.00^{e}	0.00^{e}	0.00^{e}	0.00^{e}
LSD	9.72	8.86	7.11	10.05

*Means in a column followed by the same letter are not significantly different (ANOVA, P < 0.05)

The calculated LC50 and LC90 values of ***C1*** and ***C2*** against mycelial growth of two plant pathogenic fungi are shown in Table 8 and 9. The chemicals had an obvious inhibitory activity against both test fungi, and the LC 50 values ranged from 4.598 µg/mL to11.708 µg/mL and LC90 values ranged from 21.134µg/mL to 33.603µg/mL. The LC90 of the inhibition of ***C1*** and ***C2*** against mycelial growth of *A. solani* were 33.371 µg/mL and 33.603 µg/mL respectively. On the other hand, the LC90 of the inhibition of ***C1*** and ***C2*** against mycelial growth of *R. solani* were 21.134 µg/mL and 31.677 µg/mL respectively. These results indicate that ***C1*** and ***C2*** have a potential in control of these fungi (Table 9).

(Insert Table 9 here)

3.7. Anticancer Activity

3.7.1. Antiproliferative effect of C1 and C2 against HT-29, HeLa, C6 and Vero cell lines

The antiproliferative effect of ***C1*** and ***C2*** against HT-29, HeLa, C6 and Vero cells was determined using BrdU Cell Proliferation ELISA assay. In contrast to control compound, *5FU*, both ***C1*** and ***C2*** were significantly inhibited proliferation of HeLa ($p<0.05$), C6 ($p<0.05$), and HT-29 ($p<0.05$) cells (Fig. 6). However, antiproliferative activity both complexes were significantly ($p<0.05$) lower against Vero cells (Fig. 6). IC_{50} concentrations of ***C1***, ***C2***, $[Ag(CN)_2]^{1-}$ and *5FU* were given in Table 10.

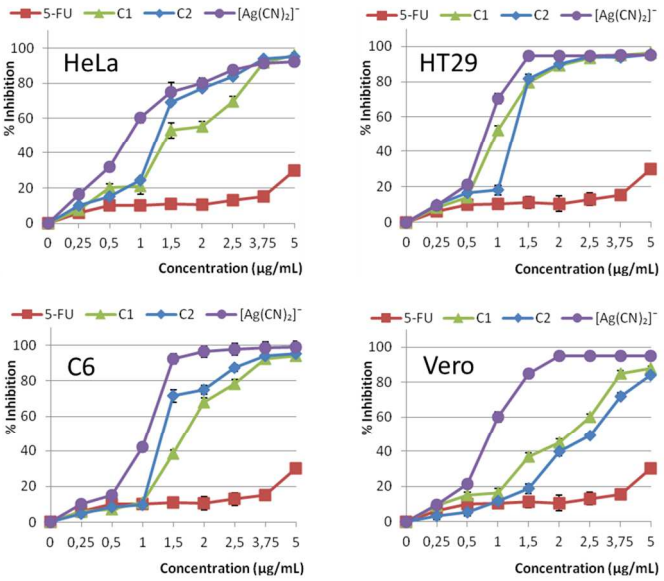

Figure 6. Effects of ***C1***, ***C2*** and $[Ag(CN)_2]^{1-}$ on the proliferation of HT-29, HeLa, C6 and Vero cell lines. Exponentially growing cells

were incubated with ***C1***, ***C2*** and $[Ag(CN)_2]^{1-}$ for 24 hours and the cell proliferation was measured by the BrdU Cell Elisa assay. Percent inhibition was reported as mean values ± SEM of three independed assays.

(Insert Table 9 here)

3.7.2. *Cytotoxic activity of C1 and C2 on HT-29, HeLa, C6 and Vero cell lines*

The cytotoxic activity of ***C1*** and ***C2*** in HT-29, HeLa, C6 and Vero cells were tested by LDH cytotoxicity assay. The percent cytotoxicity of ***C1***, ***C2***, and *5FU* were ranged from 15 % to 25 % whereas, $[Ag(CN)_2]^{1-}$ showed about 60% cytotoxicity ($p < 0.05$) against all cell lines. The results showed that cytotoxicity of both compounds were closed to cytotoxicty of *5FU* at their IC_{50} concentrations on the cells tested. Therefore, It is suggested that these compounds may have cytostatic potential rather than cytotoxic potential. The significantly lower cytotoxicity of ***C1*** and ***C2*** than $[Ag(CN)_2]^{1-}$ alone may indicate that cytotoxicity of $[Ag(CN)_2]^{1-}$ decreased to safe leves when complexed with N-(2-hydroxyethyl) ethylenediamine in the ***C1*** and ***C2*** without reducing their antiproliferative potential (Figure 7).

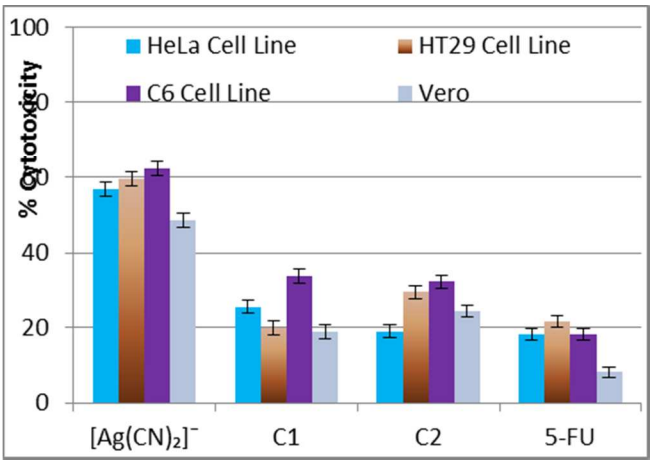

Figure 7. Cytotoxic activity of ***C1***, ***C2*** and $[Ag(CN)_2]^{1-}$ on HT-29, HeLa, C6 and Vero cell lines. Exponentially growing cells were incubated with IC_{50} concentrations of ***C1***, ***C2*** and $[Ag(CN)_2]^{1-}$ and cytotoxicity was determined by LDH Cytotoxicity Assay. Cytotoxicity of ***C1***, ***C2*** was siginificantly ($p < 0.05$) lower than $[Ag(CN)_2]^{1-}$. Percent cytotoxicity was reported as mean values ± SDs of three independed assays.

3.7.3. *Detection of apoptotic potential of C1 and C2 by DNA laddering Assay*

In the present study, to test whether the mechanism of antiproliferative and cytotoxic activity of ***C1*** and ***C2*** involves apoptosis, we determined DNA laddering potential of ***C1*** and ***C2*** on HeLa, HT29 and C6 cell lines. The DNA laddering assay results showed that both coordination compounds caused fragmentation of DNA, indicating that these compounds act by inducing apoptosis (Fig. 8). These results were parallel to antiproliferative and cytotoxic activityies ***C1*** and ***C2***.

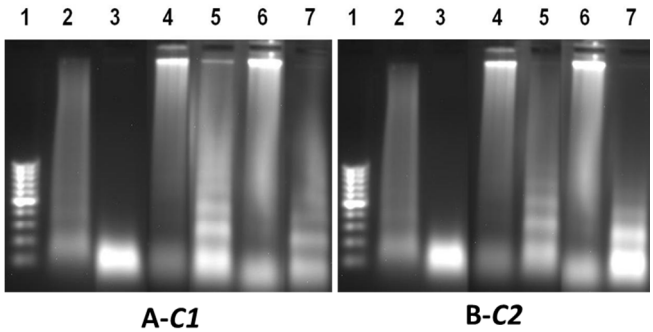

Figure 8. Effects of ***C1*** and ***C2*** on DNA fragmentation. Exponentially growing HeLa, C6 and HT-29 cells were incubated with ***C2*** at 37°C for overnight, DNA isolated and DNA fragmentation was visualized by agarose gel electrophoresis. Both ***C1*** and ***C2*** were caused DNA fragmentation. (A-***C1***: Lane 1, DNA standard; Lane 2, HeLa Control; Lane 3, HeLa+***C1***; Lane 4, HT29 Control; Lane 5, HT29+***C1***; Lane 6, C6 Control; Lane 7, C6+***C1***. B-***C2***: Lane 1, Marker; Lane 2, HeLa Control; Lane 3, HeLa+***C2***; Lane 4, HT29 Control; Lane 5, HT29+***C2***; Lane 6, C6 Control; Lane 7, C6+***C2***).

3.7.4. *Detection of apoptotic potential of C1 and C2 by TUNEL assay*

We performed TUNEL assay to investigate whether ***C1*** and ***C2*** inhibit cell proliferation by apoptosis. HT29 cell lines were incubated with IC_{50} concentrations of ***C1*** and ***C2*** for overnight and apoptosis was detected using TUNEL assay. As shown in Figure 9A and D, HT29 cells treated with ***C1***, ***C2*** and *5FU* showed green fluorescence, indicating the fragmented DNA in apoptotic cells, whereas no apoptotic signal was observed in the cells treated with DMSO (Fig 9C).

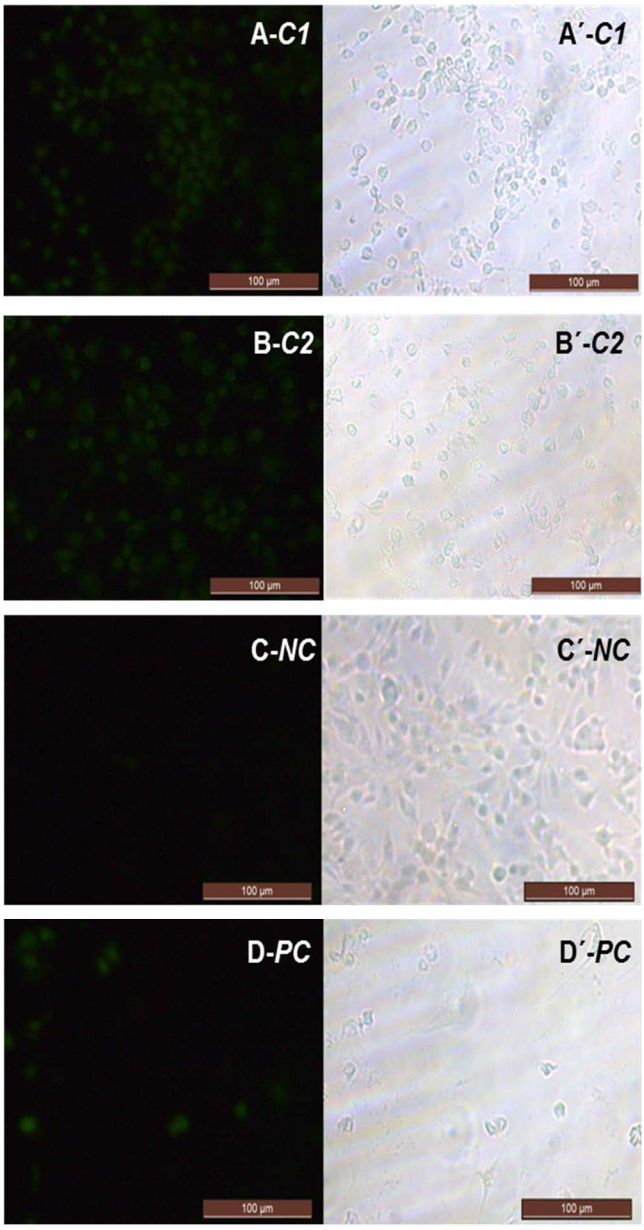

Figure 9. Fluorescence and phase-contrast images of the HT29 cancer cell line examined by TUNEL assay. TUNEL-positive cell nuclei with brilliant green were observed under a fluorescence (A, B, C, and D) and phase-contrast microscope (A′, B′, C′, and D′). C1 and C2: treatments, NC: negative control,PC: positive control).

3.7.5. *Detection of migration inhibitory activity of C1 and C2*

Migration of the cancer cells is very important characteristics and an excellent drug target for the migrating cancer cells resistant to apoptosis. The migration inhibitory effect of ***C1*** and ***C2*** on HeLa cell lines was investigated using migration assay. It is found that ***C1*** and ***C2*** at IC_{50} concentrations showed suppressive effect on the migration of HeLa cell line in a time-dependent manner (Fig. 10A, B). It is suggested that ***C1*** and ***C2*** may have antimetastatic potential.

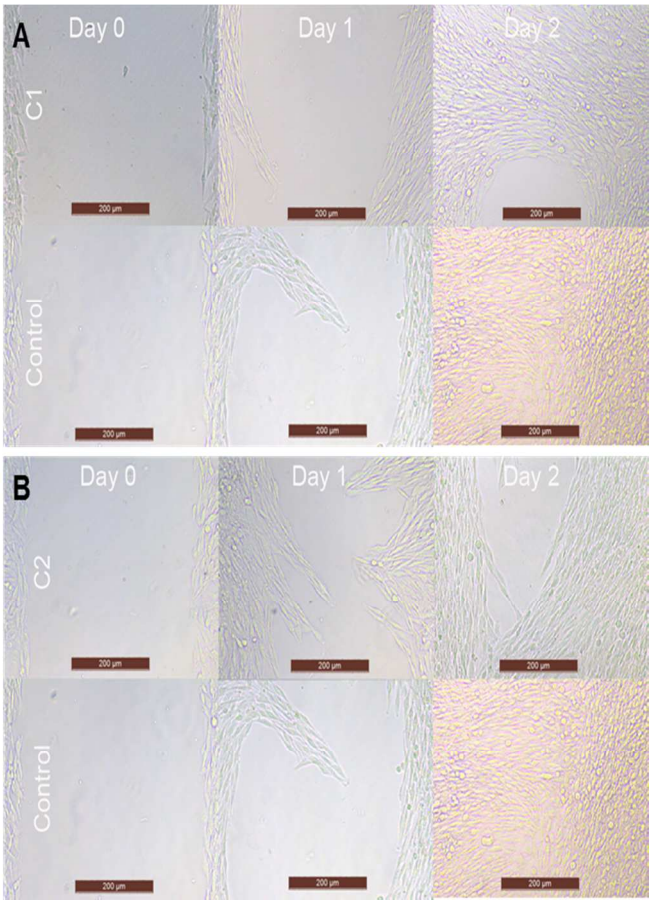

Figure 10. Effect of ***C1*** and ***C2*** on the migration of HeLa cell line. The closure of the HeLa cell line was photographed 0, 1 and 2 days after incubation with ***C1*** (A) and ***C2*** (B) at IC_{50} concentrations using a phase contrast microscope (Leica DMIL, Germany) until complete cell closure was observed in the untreated control. Note that antimigration effect of ***C1*** and ***C2*** on the cells was more obvious at day 2.

3.7.6. *Detection of DNA topoisomerase I inhibitory activity of C1 and C2*

DNA topoisomerase I is a nuclear enzymes that play essential roles in controlling the topological state of DNA to facilitate and remove barriers for vital cellular functions including DNA replication and repair. Therefore, DNA topoisomerase I is an important target for anti-cancer agents. DNA topoisomerase I inhibitory activity of ***C1*** and ***C2*** was investigated using Topoisomerase inhibition assay. It is found that ***C1*** and ***C2*** at IC_{50} concentrations inhibited activity of recombinant human DNA Topoisomerase I as positive control, Camptothecine (Fig. 11). This result may indicate that the compounds inhibit cell proliferation by the suppression of DNA Topoisomerase I action during replication. Since DNA Topoisomerase I is an important enzyme for bactrerial replication, It is suggested that antibacterial activity of these compounds may involve inhibition of bacterial DNA Topoisomerase I.

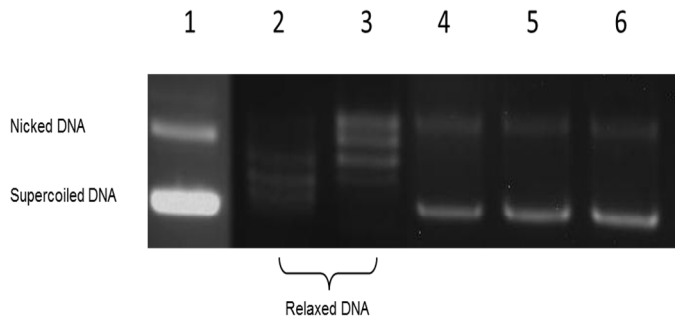

Figure 11. Inhibition of recombinant human topoisomerase I activity by ***C1*** and ***C2***. The super coiled plasmid DNA was incubated with DNA topoisomerase I only and DNA topoisomerase I plus ***C1*** and ***C2*** and Camptothecin. The results showed that ***C1, C2*** and Camptothecin inhibited DNA relaxing activity of DNA topoisomerase I. Lane 1: Supercoiled marker DNA; Lane 2: Relaxed marker DNA; Lane 3: Negative Control (Supercoiled DNA + Topo I); Lane 4: Positive Control (Supercoiled DNA + Topo I + Camptothecin); Lane 5: Supercoiled DNA + Topo I + ***C1***; Lane 6: Supercoiled DNA + Topo I + ***C2***.

Cancer is the most common disease and affected more than 14.1 million people in 2012 in the world [55]. The cervical, colon and brain cancers are very common cancers after breast cancer worldwide [55]. Therefore, development of novel and safer drugs are necessary to cure these cancers. In addition, the use of appropriate cell lines, particularly for antiproliferative and cytotoxic studies, is very important. Thus, we used HeLa, HT29, C6 tumor cell lines for *in vitro* anticancer studies.

In recent years, biological activities of various metal coordination complexes have been studied [56-61] Platinum containing complexes such as c*is*-platinum and its derivatives are the most studied metal complexes with anticancer activity [62-63]. However, anticancer activities of many novel non platinum complexes such as Ag^{I} complexes are unknown [64-68]. In the present study, antiprolifrative and cytotoxic activities of ***C1*** and ***C2*** containing $[Ag(CN)_2]^{1-}$ were tested on HeLa, HT29, C6 and Vero cell lines using BrdU cell proliferation ELISA assay. Antiproliferative activity of both compounds on Hela, HT29 and C6 tumor cell lines were significantly higher ($p < 0.05$) than *5FU* (Fig. 6), wheras they showed significantly lower ($p < 0.05$) antiproliferative effect on Vero cell line.(Fig. 6). In addition, cytotoxicity of ***C1*** and ***C2*** were lower on all cell lines including Vero Cells and substantially closed to cytotoxicty of *5FU*. Because of their low cytotoxicity on tumor cells, it is suggested that ***C1*** and ***C2*** may posses cytostatic potential rather than cytotoxicity (Fig. 7). Further tests indicated that cytotoxicity of ***C1*** and ***C2*** was concentration dependent (data not shown). It may be thought that $[Ag(CN)_2]^{1-}$ contributes to antiproliferative and cytotoxicity activities of the complexes. Indeed, the antiproliferative activity of complexes and $[Ag(CN)_2]^{1-}$ on the cell lines tested were almost same. However, cytotoxicity of complexes were significantly lower than that of $[Ag(CN)_2]^{1-}$ alone (p<0.05) (Fig. 7) indicating their high antipropliferative potential with low cytotoxicty. Although $[Ag(CN)_2]^{1-}$'s very obvious contribution on the antiproliferative activities of these complexes, it is very clear that they are very important compounds with their high antiproliferative and low cytotoxic potential. These results were somewhat similar to previous studies such as Zachariadis [69], El-din [70], Korany [71], Pettinari [72], Banti [73].

Furthermore, the results of DNA laddering (Fig. 8) and TUNEL assays (Fig. 9) indicated that ***C1*** and ***C2*** were actualy inhibit proliferation of HT29 cell line through induction of apoptosis. In addition, these compounds were inhibited migration of HeLa cells (Fig. 10), indicating their antimetastatic potential. DNA topoisomerase I is an important antitumor target because of their essential physiological functions regulating DNA topology during DNA replication and recombination. Since ***C1*** and ***C2*** showed antiproliferative and antibacterial activity, we have tested whether they posses topoisomerase I inhibitory activity. Results revealed that IC_{50} concentration of ***C1*** and ***C2*** inhibited almost all the relaxation activity of topoisomerase I (Fig. 11).

Based on our results, it is suggested that these complexes have important biological activities. Because of their impressive antiproliferative, cytostatic, antimigratory and antitopoisomerase activities, we suggested that ***C1*** and ***C2*** are potential and valuable anticancer drug candidates to be used in medicine. Although, the ***C1*** and ***C2*** possess very significant anticancer activity *in vitro*, their activity *in vivo* are unknown. Therefore, *in vivo* anticancer activity and the mechanism of induction of apoptosis of these novel complexes need further studies.

IV. Conclusions

Cd^{II} and Ni^{II} centered bimetallic silver (or argentate) complexes were synthesized by mixing metal chlorides and *hydeten* with $K[Ag(CN)_2]$. These complexes were characterized by various spectroscopic and analaysis methods. *FT-IR* spectra of these complexes pointed out that cyanido bridges formed in both ***C1*** and ***C2*** have also terminal cyanido groups. According to *X*-ray spectra, ***C2*** consists of $[Cd(hydeten)_2]^{2+}$ units, of which Cd^{II} exhibits an octahedral geometry bridged by $[Ag(CN)_2]^{1-}$ anions. A unique feature of ***C2*** is to exhibit the first example of oligocyanidoargentate anion $[Ag(CN)_2]_n^{n-}$ (n= 3) assembled through ligand-unsupported d^{10}–d^{10} interactions in the solid state. The thermal decomposition behaviors of both complexes were understood to follow the usual pattern in which first neutral and then anionic ligands are liberated even though decomposition stages were not fully identified. According to our results both complexes exhibited very strong antimicrobial, antifungal and anticancer activities. Comparison of the cytotoxicty of $[Ag(CN)_2]^{1-}$ with the cytotoxicties ***C1*** and ***C2***, has clearly shown the importance of anticancer activities of these novel complexes.

Acknowledgements

The authors thank the Scientific and Technical Research Council of Turkey (TUBİTAK, Grant TBAG-112T696; COST Action CM 2515) and the Gaziosmanpaşa University Research Foundation (Grant 2011/32) for financial support.

Notes and references

[a]*Department of Chemistry, Art and Science Faculty, Gaziosmanpaşa University, 60250, Tokat, TURKEY. Fax: +90(356)2521585; Tel: +90(356)2521616; Ahmet Karadağ: ahmet.karadag@gop.edu.tr; akaradag68@gmail.com Nesrin Korkmaz: nesrinokumus@gmail.com*

[b]*Department of Molecular Biology and Genetics,, Art and Science Faculty, Gaziosmanpaşa University, 60250, Tokat, TURKEY. Fax: +90(356)2521585; Tel: +90(356)2521616; Şaban Tekin: sabant@yahoo.com; Ali Aydın: aliaydin.bio@gmail.com*

[c]*Department of Plant Protection, Faculty of Agriculture, Gaziosmanpaşa University, 60240, Tokat TURKEY. Fax: +90(356)2521585; Tel: +90(356)2521616; Yusuf Yanar; yusuf.yanar@gop.edu.tr*

[d]*Department of Bioengineering, Engineering and Natural Science Faculty, Gaziosmanpaşa University, 60240, Tokat TURKEY. Fax: +90(356)2521585; Tel: +90(356)2521616; İsa Karaman; isa.karaman@gop.edu.tr*

† X-ray crystallographic files in CIF format for ***C2***, crystallographic data for the structure reported here has been deposited with the Cambridge Crystallographic Data Centre as supplementary data, CCDC Nos. 905446. Copies of the data can be obtained through application to CCDC, 12 Union Road, Cambridge CB2 1EZ, UK. (Fax: +44 1223 336033 or e-mail: deposit@ccdc.cam.ac.uk or at http://www.ccdc.cam.ac.uk).

References

1 W. Dong, Q.-L. Wang, S.-F. Si, D.-Z. Liao, Z.-H. Jiang, S.-P. Yan, P. Cheng, Inorg. Chem. Commun., 2003, **6**, 873.
2 A. J. Blake, N. R. Champness, P. Hubberstey, W. S. Li, M. A. Withersby, M. Schroder, Coord. Chem. Rev., 1999, **183**, 117.
3 D. B. Leznoff, B.-Y. Xue, R. J. Batchelor, F. W. B. Einstein, B. O. Patrick, Inorg. Chem., 2001, **40** (23), 6026.
4 (a) D. N. Reinhoudt, J. F. Stoddart, R. Ungaro, J. Eur. Chem. 1998, **4**, 1349; (b) J. K. M. Sanders, J. Eur. Chem., 1998, **4**, 1378.
5 P. J. Hagnan, D. Hagrman, J. Zubieta, Angew. Chem. Int. Ed. Engl., 1999, **38**, 2638.
6 A. N. Khlobystov, A.J. Blake, N.R. Champness, D.A. Lemenovskii, A.G. Majouga, N.V. Zyk, M. Schröder, Coord. Chem. Rev., 2001, **222**, 155.
7 P. Pyykkö, Chem. Rev., 1997, **97**, 597.
8 D. M. Pham, D. Rios, M. M. Olmstead, A. L. Balch, Inorg. Chim. Acta., 2005, **358**, 4261.
9 C. S. Shaw III, Chem Rev., 1999, **99**, 2589.
10 J. -Y. Wang, W. Gu, W. -Z. Wang, X. Lıu, D. -Z. Lıao, Chem. Res. Chinese U., 2006, **22**, 283.
11 C.-M. Che, M.-C. Tse, M.C.W. Chan, K.-K. Cheung, D.L. Phillips, K.-H. Leung, J. Am. Chem. Soc., 2000, **122**, 2464.
12 L′. Triscikova, I. Potočňák, J. Chomič, Transit. Metal Chem., 2003, **28**, 808.
13 T. Soma, T. Iwamoto, Chem.Lett., 1994, 821.
14 T. Soma, T. Iwamoto, Inorg. Chem., 1996, **35**, 1849.
15 M.A. Omary, T.R. Webb, Z. Assefa, G.E. Shankle, H.H. Patterson, Inorg. Chem., 1998, **37**, 1380.
16 T.Soma, H. Yuge, T. Iwamoto, Angew. Chem. Int. Ed. Engl., 1994, **33**, 1665.
17 L′. Triscikova, I. Potočňák, C. Wagner, Acta Cryst., 2002, **C58**, m246.
18 T. Iwamoto, J. Inclusion, Phenom. Mol. Recognit. Chem., 1996, **24**, 61.
19 T. Soma, T. Iwamoto, Mol. Cryst. Liq. Cryst., 1996, **276**, 19.
20 I. Dasna, S. Golhen, L. Ouahab, N. Daro, J.P. Sutter, Polyhedron, 2001, **20**, 1371.
21 V. Comte, Z.-N. Chen, M.-L. Flay, H. Vahrenkamp, J. Organometal. Chem., 2000, **614-615**, 131.
22 I.P.Y. Shek, W.-Y. Wong, T.C. Lau, New J. Chem., 2000, **24**, 733.
23 Z. Assefa, R.J. Staples , J.P. Fackler, Jnr, H. H. Patterson, G. Shankle, Acta Cryst., 1995, **C51**, 2527.
24 J. Chomič, J. Černák, I. Potočňák, I. Zvereva, N. Savelieva, Chem. Papers., 1993, **47**, 175.
25 J. Chomič, J. Černák, J. Grigl'áková, J. Therm. Anal., 1988, **33**, 661.
26 J. Chomič, J. Černák, Thermochim. Acta, 1985, **93**, 93.
27 A. Karadağ, H. Paşaoğlu, G. Kaştaş, O. Büyükgüngör, Acta Crystallogr., 2004, **C60**, m581.
28 A. Karadağ, A. Bulut, O. Büyükgüngör, Acta Crystallogr., 2004, **C60**, m402.
29 A. Karadağ, H. Paşaoğlu, G. Kaştaş, O. Büyükgüngör, Z. Kristallogr., 2005, **220**, 74.
30 A. Karadağ, Z. Kristallogr., 2007, **222**, 39.
31 A. Karadağ, İ. Önal, A. Şenocak, İ. Uçar, A. Bulut, O. Büyükgüngör, Polyhedron, 2008, **27**, 223.
32 H. Paşaoğlu, A. Karadağ, F. Tezcan, O. Büyükgüngör, Acta Crystallogr., 2005, **C61**, m93.
33 Rigaku, *Crystal-Clear*, Version 1.3.6; Rigaku American Corporation 9009 New Trails Drive, The Woodlands, TX 77381-5209, USA, 2005.
34 Sheldrick, G. M., SHELXS97 and SHELXL97, University of Göttingen, Germany, 1997.
35 P. R. Murray, E. J. Baron, M. A. Pfaller, F. C. Tenover, R. H. Yolke, *Manual of Clinical Microbiology,* vol. 6, ASM, Washington, DC 1995.
36 J. R. Zgoda, J. R. Porter, *Pharmaceutical Biology.,* 2001, **39**, 221.
37 L. Boyanova, G. Gergova, R. Nikolov, S. Derejian, E. Lazarova, N. Katsarov, I. Mitov, Z. Krastev, *J. Medical Microbiology*., 2005, **54**, 481.
38 C. A. Berkeley, Leora Software, 1994.
39 M. Tripathi, N. K. Dubey, A. K. Shukla, *World J. Microbiol Biotechnology,* 2008, **24**, 39.

40 J. Gong, F. Traganos, Z. Darzynkiewicz., *Anal. Biochem*., 1994, **218**(2), 314.
41 J. Černák, M. Orendáč, I. Potočňák, J. Chomič, A. Orendáčová, J. Skoršepa, A. Feher, *Coord. Chem. Rev*., 2002, **224**, 51.
42 K. Nakamato, *Infrared and raman spectra of inorganic and coordination compounds* Part B; A John Wiley & Sons, Inc., Publication, USA, 2009, p. 110.
43 L′. Triscikova, I. Potočňák, J. Chomič, T. Müller, *Thermochim. Acta,* 2004, **419**, 231.
44 B.H. Stuart, *Infrared spectroscopy: fundamentals and applications*; Wiley Interscience Publication, New York, 2004.
45 A. Karadağ, A. Bulut, A. Şenocak, İ. Uçar, O. Büyükgüngör, *J. Coord. Chem.,* 2007, **60**, 2035.
46 J. Černák, J. Skoršepa, J. Chomič, I. Potočňák, J. Hoppan, *J. Therm. Anal.,* 1994, **41**, 91.
47 H. Zhang, J. Cai, X.-L. Feng, T. Li, X.-Y. Li, L.-N, Ji, *Inorg. Chem. Commun.* 2002, **5**, 637.
48 L′. Triscikova, J. Chomic, K:A:Abbound, J.-H. Park, M.W. Meisel, J. Cernak, *Inorg. Chem.* 2004, **357**, 2763.
49 J. Černák, I. Potočňák, J. Chomič, *J. Therm. Anal*., 1993, **39**, 849.
50 J. Černák, J. Chomič, I. Potočňák, *J. Therm. Anal*., 1989, **35**, 2265.
51 V. T. Yılmaz, A. Karadağ, *Thermochim. Acta,* 2000, **348**, 121.
52 F. Yakuphanogğlu, A. Karadağ, M. Şekerci, *J. Therm. Anal*., 2006, **86**, 727.
53 J. J. Earney, C.P.B. Finn and B. M. Najafabadi, *J. Phys. C: Solid St. Phys*., 1971, **4**,1013.
54 B. J. Hathaway, D. E. Billing, *Coord. Chem. Rev*., 1970, **5**, 143.
55 Forman D, Bray F, Brewster DH, Gombe Mbalawa C, Kohler B, Piñeros M, Steliarova-Foucher E, Swaminathan R and Ferlay J, Cancer Incidence in Five Continents, Vol. X (electronic version) Lyon, IARC. http://ci5.iarc.fr, (2013)
56 D. Fregona, L.Ronconi, D. Aldinucci, *Drug Discov. Today*, 2009, **14**(21), 1075.
57 A. Kastl, A.Wilbuer, A. L. Merkel, L. Feng, P. D. Fazio, M.Ocker, E.Meggers, *Chem. Commun*. 2012, **48**, 1863.
58 I. Ott, R. Gust, *Anticancer Agents Med Chem*., 2007, **7**(1), 95.
59 L. Ronconi, P. J. Sadler, *Coord. Chem. Rev.,* 2007, **251**, 1633.
60 B. S. Creaven, E. Czeglédi, M. Devereux, É.A. Enyedy, A. Foltyn-Arfa Kia, D. Karcz, A.Kellett, S. McClean, N.V. Nagy, A. Noble, A. Rockenbauer, T.Szabó-Plánka, *Dalton Trans*., 2010, **7**, 39(45) 10854.
61 L. Cattaruzza, D. Fregona, M. Mongiat, L. Ronconi, A. Fassina, A. Colombatti, D. Aldinucci, *Int. J. Cancer*, 2011, **128**(1), 206.
62 L.Kelland, *Nat. Rev. Cancer,* 2007, **7**(8), 573.
63 J. Reedijk, *Platinum Metals Rev.,* 2008, **52** (1), 2.
64 M.A. Iqbal, R.A. Haque, S.T. Nasri, A.A. Majid, M.B.K. Ahamed, E. Farsi, T. Fatima, Chem. Cent. J. 2013 **(1)**, 27.
65 D.A. Medvetz, K.M. Hindi, M.J. Panzner, A.J. Ditto, Y.H. Yun, W.J. Youngs, Met. Based. Drugs. 2008, 384010.
66 B. Thati, A. Noble, B.S. Creaven, M. Walsh, M. McCann, M. Devereux, K. Kavanagh, D.A. Egan, Eur. J. Pharmacol. 2009, **602**(2-3), 203.
67 S.K. Hadjikakou, I.I. Ozturk, M.N. Xanthopoulou, P.C. Zachariadis, S. Zartilas, S. Karkabounas, N. Hadjiliadis N, J. Inorg. Biochem. 2008, **102**(5-6), 1007.
68 V. Gandin, M. Pellei, M. Marinelli, C. Marzano, A. Dolmella, M. Giorgetti, C. Santini. J. Inorg. Biochem. 2013, **129**, 135.
69 P. C. Zachariadis, S. K. Hadjikakou, N. Hadjiliadis, S. Skoulika, A. Michaelides, J. Balzarini, E. D. Clercq, *E. J. Inorg. Chem.*, 2004, **7**, 1420.
70 El-D. H. E. Safaa, A. S. Sultan, A.S. Badr El-Din, *Eur. J. Med. Chem.,* 2011, **46**(11), 5370.
71 A. A. Koray, Abd-E. M. Mokhles, M. Khaled, *Inter. J. Medicinal Chem.,* 2013, 1.
72 C. Pettinari, F. Marchetti, G. Lupidi, L. Quassinti, M. Bramucci, D. Petrelli, L. A. Vitali, M. F. da Silva, L. M. Martins, P. Smoleński, A. J. Pombeiro. *Inorg Chem*., 2011, *7* **50**(21), 11173.
73 C. N. Banti, S.K. Hadjikakou, *Metallomics*, 2013, **5**, 569.

New Journal of Chemistry RSCPublishing

ARTICLE

Table 5. Thermoanalytical data for ***C1*** and ***C2***

Complex	Stage	Temperature Range (°C)	DTG_{max} (°C)	ΔH (J/g)	Mass loss, Δm (%)		Total mass loss, Δm (%)		Removed group
					Found.	Calc.	Found.	Calc.	
$C_{12}H_{26}N_8O_3Ag_2Ni$(***C1***) MA: 604,82	1	35-194	93	-282,87	2,93	37.39	2,93	37.39	H_2O + *2hydeten*
	2	194-266	240	-419,31	17,58		20,51		
	3	266-532	321	-487,92	17,31		37,82		
	4	532-825	740	210,81	16,89	17,20	54,71	54,59	4CN
$C_{16}H_{24}N_{12}O_3Ag_4Cd_2$(***C2***) MA: 1088,75	1	35-71	46	20,47	1,62	1,65	1,62	1,65	H_2O
	2	71-150	91	36,54	3,08	19,10	4,70	20,76	2*hydeten*
	3	150-367	253	-321,47	16,82		21,52		
	4	367-700	798	-590,25	10,75		32,27		
	5	700-903	1014	-132,36	11,12	39.65	43,39	60,40	8 CN + 2 Cd
	6	903-1195	1132	256,94	17,88		61,27		

Table 9. Summary of probit analysis parameters of the dose-response test performed with ***C1*** and ***C2*** against two plant pathogenic fungi (*Alternaria solani* and *Rhizoctonia solani*)

Bioassay	Slope (±SE)	LC50 (95% of fiducial limits)	LC90 (95% of fiducial limits)	$\chi 2^c$
A. solani	1.499±0.198[a]	4.658(3.541-5.652)	33.371(24.066-56.677)	7.163
	1.484±0.198[b]	4.598(3.472-5.597)	33.603(24.148-57.531)	7.296
R. solani	4.997±0.415[a]	11.708(10.924-12.552)	21.134(18.887-24.674)	21.773
	2.552±0.240[b]	9.968(8.999-11.067)	31.677(25.741-42.381)	14.006

[a]Slope of the concentration (±standard error) response of the fungi to ***C1***
[b]Slope of the concentration (±standard error) response of the fungi to ***C2***
[c]Pearson chi-square goodness-of-fit test on the probit model (α=0.05)

Table 10. IC_{50} concentrations of ***C1***, ***C2***, $[Ag(CN)_2]^{1-}$ and 5FU

	HeLa Cell Line (μg/mL)	HT29 Cell Line (μg/mL)	C6 Cell Line (μg/mL)	Vero Cell Line (μg/mL)
C1	1.43	0.96	1.45	1.33
C2	1.19	1.08	1.22	1.64
$[Ag(CN)_2]^{-1}$	1.02	1.03	1.01	1.12
5FU	35.86	33.62	28.29	35.42